Direct-gap photoluminescence from germanium nanowires

Yoko Kawamura,[3] Kevin C. Y. Huang,[1] Shruti V. Thombare,[1] Shu Hu,[1] Marika Gunji,[1] Toyofumi Ishikawa,[3] Mark L. Brongersma,[1,2] Kohei M. Itoh,[3] and Paul C. McIntyre[1,2,*]

[1]*Materials Science and Engineering, Stanford University, Stanford, California 94305*

[2]*Geballe Laboratory for Advanced Materials, Stanford University, Stanford, California 94305*

[3]*School of Fundamental Science and Technology, Keio University, 3-14-1 Hiyoshi, Kohoku-ku, Yokohama 223-8522, Japan*

(Received 15 March 2012; published 6 July 2012)

We report observation of near-infrared photoluminescence from free-standing, vertically aligned germanium nanowires grown on a (111)-oriented silicon substrate. The energy of the photoluminescence peak is very close to that of the bulk crystalline germanium direct band gap. The intensity shows an approximately quadratic dependence on excitation laser power and decreases with decreasing temperature. The peak position exhibits a redshift with increasing laser power due to laser-induced heating of the wires. These observations indicate that the photoluminescence originates from the direct band-gap recombination in the germanium nanowires.

DOI: 10.1103/PhysRevB.86.035306 PACS number(s): 78.67.Uh

I. INTRODUCTION

Over the last decade, nanoscale semiconductor structures with low dimensionality (D) such as quantum wells (2-D), nanowires (NWs; 1-D), and nanocrystals (0-D) have attracted much attention due to their remarkable physical properties and possible applications in nanoscale electronic and optoelectronic devices.[1,2] In particular, Ge nanostructures open the possible use of indirect band-gap semiconductors as materials for new nanoscale optoelectronic devices, primarily thanks to their high carrier mobilities, strong photon absorption, and compatibility with modern silicon integrated circuits. Therefore, the photoluminescence (PL) properties of such Ge nanoscale structures are of great interest. There have been several reports on the observation of near-infrared (NIR) PL from Ge quantum wells.[3–7] For lower-dimension structures, recent developments have mainly concerned visible PL from Ge nanocrystals embedded in various oxide matrices.[8–13] The origin of the observed blue PL has been discussed extensively and is attributed to defects at the nanocrystal-matrix interface or in the matrix itself. In addition, NIR PL due to radiative recombination of quantum-confined carriers in Ge nanocrystals embedded in silicon dioxide matrices,[14] wire-shaped Ge islands grown on Si substrates,[15] and Ge quantum wires self-aligned at step edges on Si[16] has been reported.

For Ge NWs, Audoit *et al.*[1] have measured ultraviolet (UV) PL from Ge NWs encased within mesoporous silica. In this case the strain imposed on the wires by the matrix may have induced the UV PL in the NWs. On the other hand, despite the great number of reports on light-emitting indirect band-gap Si NWs[17,18] as well as the synthesis of high-quality free-standing Ge NWs and their structural[19–21] and electrical[22,23] characterization, light emission from free-standing Ge NWs has not been reported before. Kamenev *et al.*[24] have tested for PL from free-standing Ge NWs grown on Si substrates in the NIR wavelength region. The Ge NWs, however, did not show a PL signal near the crystalline Ge band gap, most likely due to the presence of a high density of nonradiative recombination centers at the interface between Ge and the native oxide layer, combined with the high surface-to-volume ratio of NWs. The present paper reports, to our knowledge, the first NIR PL observations from free-standing, vertically aligned Ge NWs and discusses the origin of the observed NIR PL.

II. EXPERIMENTAL DETAILS

The two-step growth of our Ge NW samples has previously been described in Ref. 19 and will only be briefly described here. The Ge NWs used in this study were grown using colloidal gold catalyst particles of 40-nm diameter via the vapor-liquid-solid mechanism. Substrates were Si (111) (*n*-type dopant P, resistivity ranging from 1500 to 2500 Ω·cm). NW growth was carried out in a cold-walled, lamp-heated, chemical vapor deposition chamber at 375 °C (2 min, nucleation step) and 360 °C (18 min, growth step), with a GeH_4 precursor diluted with H_2. The GeH_4 partial pressure was maintained at 1 Torr in a total chamber pressure of 30 Torr for the 20-min duration of wire growth. These Ge NWs were not intentionally doped. Scanning electron microscopy (SEM) and transmission electron microscopy (TEM) were used to characterize the crystal structure, growth direction, diameter, and length of the Ge NWs. The NWs were found to be epitaxial with a ⟨111⟩ growth orientation and were single crystals. An SEM image of the Ge NWs (Fig. 1) reveals that most of these Ge NWs were vertically aligned on the Si (111) substrate with an average diameter of 40 nm and an average length of 5 μm. A fraction of the deposited NWs grow parallel to the inclined ⟨111⟩ axes of the substrates, as can be seen in Fig. 1. No dislocations were detected in the Ge NWs during TEM observations conducted in parallel with the PL study reported herein.

The samples were excited by means of a frequency-doubled Nd:YAG diode-pumped solid-state laser, emitting continuous wave at a wavelength of 532 nm (Spectra Physics Millennia Pro Laser). The emitted light was dispersed in a Spectra Pro 2750 spectrometer in the wavelength range from 1100 to 2200 nm and collected by a liquid nitrogen-cooled strained InGaAs detector. The laser beam was focused onto the sample surfaces through a 10× microscope objective having a 0.26 numerical aperture. The incident laser power on the sample surfaces was varied between 10 and 40 mW. Laser power density is ∼5 to ∼20 W/cm^2 for the investigated laser excitation power range of 10 to 40 mW. Quantum confinement effects are expected to be negligible in these NWs because the

 ©2012 American Physical Society

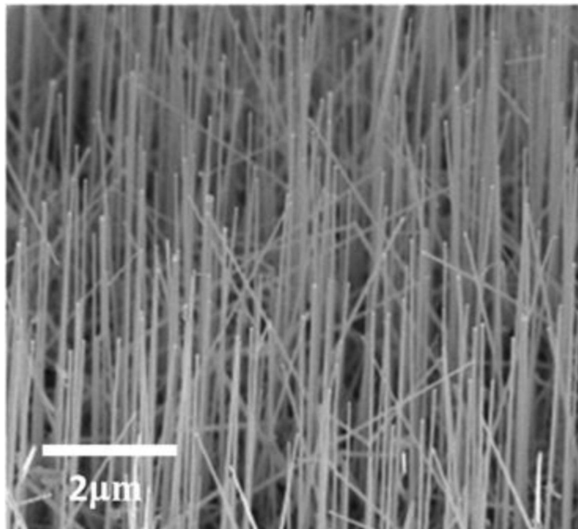

FIG. 1. SEM image, taken at a 45° tilt angle, of Au-catalyzed Ge NWs grown on a Si(111) substrate. Analysis of this image gives an average diameter and length of the Ge NWs of 40 nm and 5 μm, respectively.

diameter (~40 nm) of the NWs is larger than the exciton Bohr radius (~24 nm) of Ge.[9]

III. RESULTS AND DISCUSSION

Figure 2(a) displays the NIR room-temperature PL spectra of the Ge NWs measured with different excitation laser powers between 10 and 40 mW. The measurements were performed in air. One broad peak emerges and exhibits a monotonic shift toward longer wavelength of up to ~130 nm (~60 meV) with increasing excitation laser power. To confirm that the Si (111) substrate did not play any part in the observed PL from the Ge NWs, we performed the same experiments on a Si (111) bare substrate identical to the ones used in NW growth, with the same measurement conditions. The spectrum of the Si (111) substrate shows only one peak near the crystalline Si indirect band gap ~1.11 μm (~1.12 eV), and no other peaks are detected in the longer wavelength region. Therefore, the observed NIR PL originates from the Ge NWs. For further comparison, PL from bulk Ge [Ge (111) substrate: *p*-type dopant Ga, resistivity ranging from 1.8 to 2.3 Ω·cm] has been measured under the same conditions. As shown in the inset of Fig. 2(a), we have observed two band-edge PL peaks, corresponding to recombination through the Ge direct band gap at 1.55 μm (0.80 eV) and indirect band gap at 1.77 μm (0.70 eV) in increasing order of wavelength. Both the direct and indirect band-gap PL peak energies of the bulk Ge are insensitive to excitation laser power, in contrast to the PL peak behavior of the Ge NWs. In addition, the peaks in the inset to Fig. 2(a) are consistent with previous reports on PL from Ge.[25–33] Figure 2(b) summarizes the PL peak positions as a function of excitation laser power for both samples and shows that the PL peak energy of the Ge NWs with 10 mW laser excitation agrees with the direct band-gap PL peak energy of the bulk Ge. This agreement suggests that the observed PL from the Ge NWs originates from direct band-gap recombination.

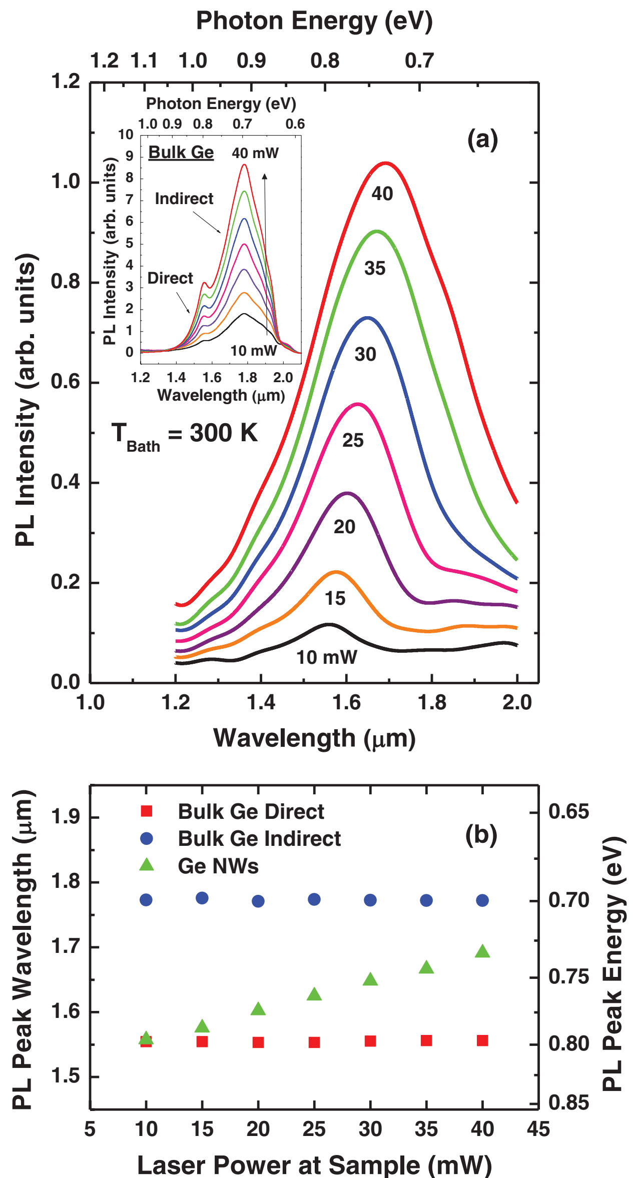

FIG. 2. (Color online) (a) NIR room-temperature PL spectra of the Ge NWs, measured at different excitation laser powers between 10 and 40 mW. The numbers below the spectra indicate the excitation laser powers incident on the sample surfaces. The inset shows the NIR room-temperature PL spectra of bulk Ge, measured under the same optical conditions as the Ge NWs. (b) PL peak wavelengths (left) and energies (right) of the bulk Ge and the Ge NWs as a function of excitation laser power at the sample surfaces.

Figure 3 displays integrated PL peak intensities as a function of excitation laser power for both samples. Note that the scale is logarithmic along both axes. For bulk Ge, the exponent is nearly equal to 1 for indirect band-gap PL and ~1.9 for direct band-gap PL. These are consistent with previously reported values.[27,29] The intensity of PL is proportional to the square of the injected carrier concentration, provided that the material is undoped, because each emitted photon is generated from a recombination event involving an excess electron-hole pair.[27] The recombination rate is then proportional to the product of the concentrations of electrons and holes, and

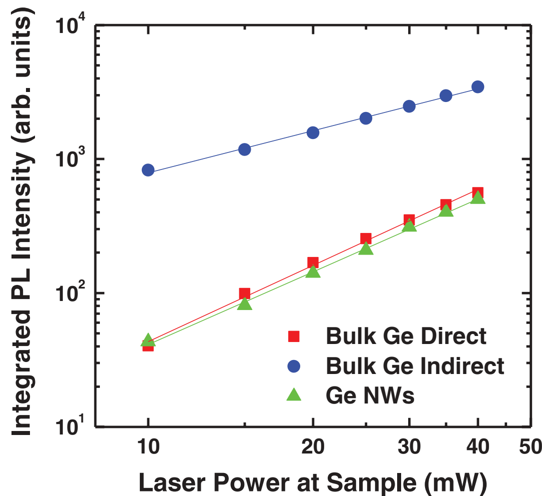

FIG. 3. (Color online) Integrated PL peak intensities of bulk Ge and the Ge NWs as a function of excitation laser power, measured at a bath temperature of 300 K (room temperature). The scale is logarithmic along both axes.

each of those is proportional to the excitation laser power.[27] The nearly quadratic dependence observed for the direct band-gap recombination from the bulk Ge matches well with the expected one. Because the concentration of electrons in the L valley of the Ge conduction band is significantly higher than that in the Γ valley, the probability of a three-carrier-mediated Auger process with energy transferred to a second electron should also be relatively high.[27,29] Auger recombination, a process that competes with nonradiative recombination, leads to a linear dependence for the case of indirect band-gap recombination in the bulk Ge.[27,29] The integrated PL peak intensity of the Ge NWs is very close to that of the direct band-gap recombination in the bulk Ge under the same measurement conditions and shows a nearly quadratic dependence on excitation laser power with an exponent of ∼1.8.

We also performed low-temperature PL measurements on both of these samples, placing them in a thermal stage (Linkam THMS600) cooled down to liquid N_2 temperature (77 K) at lowest. The measurements were conducted under N_2 atmosphere to avoid moisture condensation on the samples. Figure 4 shows the low-temperature PL spectra of (a) a bulk Ge single crystal and (b) the single-crystal Ge NW array. As shown in Fig. 4(a), with decreasing bath temperature, the indirect band-gap PL peak of the bulk Ge sharpens, and its intensity increases strongly. For direct band-gap PL in bulk Ge [see the inset to Fig. 4(a)], with decreasing bath temperature, the PL peak position shifts toward shorter wavelength, and the intensity decreases and disappears at bath temperatures below 170 K. The data in Fig. 4(a) suggest that this occurs because the direct band-gap PL is overwhelmed by the strong indirect band-gap PL. The reduction of direct band-gap PL with decreasing temperature is attributed to reduced occupancy of the Γ valley due to the sharper energy distribution of the carriers.[25,27] The PL peak from the Ge NWs has the same tendency. As shown in Fig. 4(b), with decreasing bath temperature, the PL peak position of the Ge NWs shifts toward shorter wavelength, and the intensity decreases continuously. The peak becomes unobservable at bath temperatures below 130 K. The data

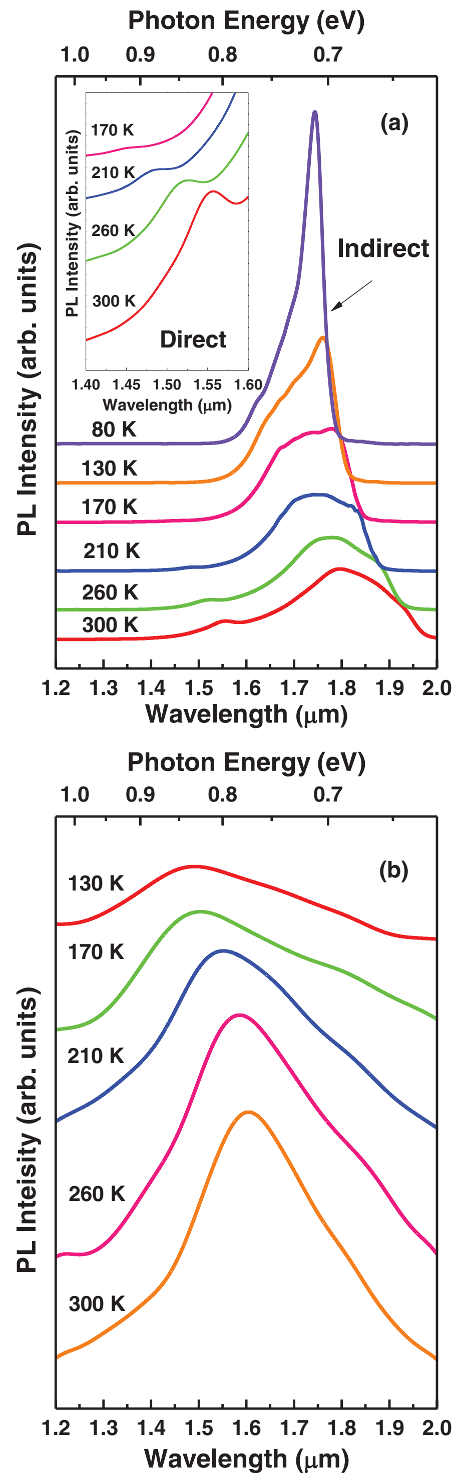

FIG. 4. (Color online) NIR PL spectra of (a) bulk Ge and (b) Ge NWs, measured at different bath temperatures. The inset to (a) shows direct band-gap PL spectra of bulk Ge in the wavelength range of 1.40 to 1.60 μm. The numbers above the spectra indicate bath temperatures. The excitation laser power incident on both samples is 40 mW.

shown in Figs. 2–4 strongly suggest that direct band-gap recombination is responsible for the PL detected from the Ge NWs. This is, to our best knowledge, the first reported experimental observation of direct band-gap PL from Ge NWs.

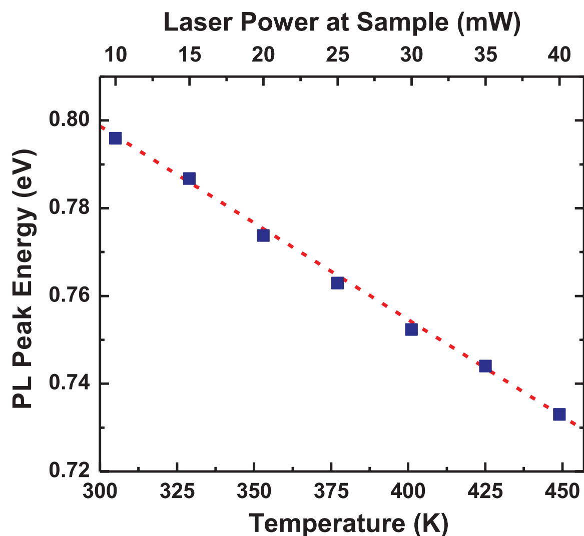

FIG. 5. (Color online) Fit of the measured PL peak energies of the Ge NWs as a function of excitation laser power at a bath temperature of 300 K (filled squares) to a linear temperature dependence of direct band-gap transitions in the bulk Ge for the temperature range 300 to 470 K (dashed line).

We now turn our attention to the origin of the redshift of the PL peaks of the Ge NWs shown in Fig. 2(a). This can be explained by laser-induced heating and subsequent heat trapping within the ensemble of dense NWs (Fig. 1). It is well known that at elevated temperatures the PL shifts toward a longer wavelength at a constant pressure due to thermal expansion of the lattice and renormalization of band-gap energies by electron-phonon interactions on the corresponding electronic states.[34–36] The latter effect gives the predominant contribution as previously demonstrated in Refs. 34–36 and will not be discussed further here. It has been reported that NW thermal conductivity can be suppressed due to phonon boundary scattering and surface roughness.[37,38] Furthermore, in a dense NW array, a fraction of the scattered PL and laser light as well as thermal radiation emitted by the NWs is confined within the array, causing ensemble heating.[39–41] This effect is not significant in bulk Ge because the PL, scattered light, and thermal radiation are more readily able to escape from the illuminated sample region to the surroundings.[39,40] Such heating effects cause the redshift and thermal broadening of the direct band-gap PL observed in our measurements of Ge NWs.

In order to estimate the temperature of the Ge NW ensemble during the PL measurements, we performed PL measurements on bulk Ge heated to temperatures between 300 and 470 K in air and estimated the approximate linear temperature coefficient for direct band-gap transitions in Ge. Our data are consistent with a value of $\Delta E/\Delta T = -4.4 \times 10^{-4}$ eV K^{-1} in this temperature range, which is also consistent with previous investigations.[34–36] Figure 5 displays the comparison of the PL peak energies of the Ge NWs as a function of excitation laser power measured at a bath temperature of 300 K and the linear temperature dependence of direct band-gap transitions in the bulk Ge. The excellent agreement also supports our conclusion that PL from the Ge NWs originates from direct band-gap recombination. These data indicate that the temperature of the Ge NWs in the illuminated arrays can reach ~450 K for the 40-mW maximum laser excitation power investigated. It is worth noting that laser-induced heating alone cannot explain the absence of indirect band-gap PL from the Ge NWs because measurements at temperatures below ~190 K did not show any significant PL signal near the indirect band-gap transition.

Several publications have previously indicated that carrier trapping at surface defects and subsequent nonradiative recombination dominates carrier relaxation in semiconductor NWs.[42–45] A thin native oxide layer forms on air-exposed Ge surfaces. The resulting surface states can be categorized as either "slow" or "fast."[45–48] Slow surface states are either in the oxide layer or on its surface, influencing carrier transport on a timescale of seconds to hundreds of seconds.[45–47] The influence of the slow surface states on carrier transport through Ge NWs has been extensively characterized in Ref. 49. In contrast, fast surface states reside at the interface between Ge and the oxide layer and are chiefly involved in recombination on a timescale of nanoseconds or less.[45–48] Carrier traps associated with fast surface states may be responsible for the failure to observe a strong PL signature for indirect band-gap recombination in the Ge NWs studied in this work. The nonradiative recombination lifetime of photogenerated carriers via GeO_x/Ge NW interface states, τ_{nrs}, can be approximated as[50,51]

$$\frac{1}{\tau_{nrs}} \cong \frac{4S}{d}, \tag{1}$$

where S is the surface recombination velocity and d is the NW diameter. Using the reported surface recombination velocity of bulk Ge with a native oxide coating, $S = 1300$ cm/s,[52] in Eq. (1), gives a value of $\tau_{nrs} \approx 1$ ns for these undoped NWs. In contrast, the radiative recombination lifetime for the indirect transition in intrinsic Ge is ~1 s, as determined by photoconductivity measurements[53] and detailed balance calculations from photon absorption data.[54] This suggests that electrons in the L valley are very likely to recombine nonradiatively in the Ge NWs prior to their radiative recombination. Both experimental[25,28] and theoretical[55] results indicate that, even if the density of occupied states in the Γ valley of intrinsic Ge is far lower than that of the L valley, the rate of direct band-gap recombination is greater for electrons near $\mathbf{k} = 0$. The data in Figs. 2–5 suggest that the rate of radiative recombination via the direct transition exceeds $1/\tau_{nrs}$ for the present NW experiments.

The direct band gap of Ge at the Γ valley is larger than its indirect band gap at the L valley by only 136 meV at room temperature, compared with the large difference between direct and indirect band gap of Si. Germanium can become a quasidirect band-gap material as a result of, for example, lattice strain. Therefore, very recently, much effort has been devoted to enhancing and controlling direct band-gap emission in bulk Ge and Ge on Si by high-concentration doping and tensile strain.[26,27,32,56–61] Our observations of direct band-gap emission from the Ge NWs are important for future Ge-NW-based optoelectronic devices and indicate that the size effect of NW diameter on nonradiative recombination rate expressed in Eq. (1) can be used to engineer important photonic properties. We expect that surface passivation of the wires through

chemical treatments, growth of a high-quality oxide layer, or growth of a semiconductor shell on the sidewalls[62] may increase the radiative-to-nonradiative recombination ratio, making Ge NWs even more attractive for future applications.

IV. CONCLUSIONS

In conclusion, we have measured NIR PL of vertically aligned, free-standing Ge NWs grown on a Si(111) substrate. The Ge NWs give one broad PL peak near the crystalline Ge band gap ∼1.55 μm (∼0.8 eV). The observed PL peak is shifted toward longer wavelengths with increasing excitation laser power due to laser-induced heating and subsequent heat trapping within the dense array of NWs. In addition, the PL peak intensity shows a nearly quadratic dependence on excitation laser power and decreases with decreasing temperature, similar to the direct band-gap PL behavior of bulk Ge crystals. These observations indicate that efficient direct band-gap recombination is responsible for the observed PL from the Ge NWs.

ACKNOWLEDGMENTS

Y.K. acknowledges a Grant-in-Aid (No. C-12) for the Global Center of Excellence program at Keio University and JSPS International Training Program (No. 21-3) at Keio University. This work has also been supported in part by NSF Grant No. DMR-0907642 and by AFOSR Grant No. FA9550-10-1-0264.

---

*Corresponding author: pcm1@stanford.edu

[1] G. Audoit, É. Ní Mhuircheartaigh, S. M. Lipson, M. A. Morris, W. J. Blau, and J. D. Holmes, J. Mater. Chem. **15**, 4809 (2005).
[2] D. M. Lyons, K. M. Ryan, M. A. Morris, and J. D. Holmes, Nano Lett. **2**, 811 (2002).
[3] J. Engvall, J. Olajos, H. G. Grimmeiss, H. Kibbel, and H. Presting, Phys. Rev. B **51**, 2001 (1995).
[4] J. Olajos, J. Engvall, H. G. Grimmeiss, M. Gail, G. Abstreiter, H. Presting, and H. Kibbel, Phys. Rev. B **54**, 1922 (1996).
[5] M. Bonfanti, E. Grilli, M. Guzzi, M. Virgilio, G. Grosso, D. Chrastina, G. Isella, H. von Känel, and A. Neels, Phys. Rev. B **78**, 041407(R) (2008).
[6] Y. Chen, C. Li, Z. Zhou, H. Lai, S. Chen, W. Ding, B. Cheng, and Y. Yu, Appl. Phys. Lett. **94**, 141902 (2009).
[7] E. Gatti, E. Grilli, M. Guzzi, D. Chrastina, G. Isella, and H. von Känel, Appl. Phys. Lett. **98**, 031106 (2011).
[8] D. C. Paine, C. Caragianis, T. Y. Kim, Y. Shigesato, and T. Ishahara, Appl. Phys. Lett. **62**, 2842 (1993).
[9] Y. Maeda, Phys. Rev. B **51**, 1658 (1995).
[10] M. Zacharias and P. M. Fauchet, Appl. Phys. Lett. **71**, 380 (1997).
[11] C. L. Yuan and P. S. Lee, Europhys. Lett. **83**, 47010 (2008).
[12] C. L. Yuan, H. Cai, P. S. Lee, J. Guo, and J. He, J. Phys. Chem. C **113**, 19863 (2009).
[13] K. S. Min, K. V. Shcheglov, C. M. Yang, H. A. Atwater, M. L. Brongersma, and A. Polman, Appl. Phys. Lett. **68**, 2511 (1996).
[14] S. Takeoka, M. Fujii, S. Hayashi, and K. Yamamoto, Phys. Rev. B **58**, 7921 (1998).
[15] M. P. Halsall, H. Omi, and T. Ogino, Appl. Phys. Lett. **81**, 2448 (2002).
[16] H. Sunamura, N. Usami, Y. Shiraki, and S. Fukatsu, Appl. Phys. Lett. **68**, 1847 (1996).
[17] A. R. Guichard, D. N. Barsic, S. Sharma, T. I. Kamins, and M. L. Brongersma, Nano Lett. **6**, 2140 (2006).
[18] O. Demichel, V. Calvo, N. Pauc, A. Besson, P. Noé, F. Oehler, P. Gentile, and N. Magnea, Nano Lett. **9**, 2575 (2009).
[19] H. Adhikari, A. F. Marshall, C. E. D. Chidsey, and P. C. McIntyre, Nano Lett. **6**, 318 (2006).
[20] H. Jagannathan, M. Deal, Y. Nishi, J. Woodruff, C. Chidsey, and P. C. McIntyre, J. Appl. Phys. **100**, 024318 (2006).
[21] T. I. Kamins, X. Li, R. S. Williams, and X. Liu, Nano Lett. **4**, 503 (2004).
[22] E. Tutuc, J. Appenzeller, M. C. Reuter, and S. Guha, Nano Lett. **6**, 2070 (2006).
[23] S. Zhang, E. R. Hemesath, D. E. Perea, E. Wijaya, J. L. Lensch-Falk, and L. J. Lauhon, Nano Lett. **9**, 3268 (2009).
[24] B. V. Kamenev, V. Sharma, L. Tsybeskov, and T. I. Kamins, Phys. Status Solidi **202**, 2753 (2005).
[25] H. M. van Driel, A. Elci, J. S. Bessey, and M. O. Scully, Solid State Commun. **20**, 837 (1976).
[26] T.-H. Cheng, K.-L. Peng, C.-Y. Ko, C.-Y. Chen, H.-S. Lan, Y.-R. Wu, C. W. Liu, and H.-H. Tseng, Appl. Phys. Lett. **96**, 211108 (2010).
[27] T. Arguirov, M. Kittler, and N. V. Abrosimov, J. Phys.: Conf. Ser. **281**, 012021 (2011).
[28] T.-H. Cheng, C.-Y. Ko, C.-Y. Chen, K.-L. Peng, G.-L. Luo, C. W. Liu, and H.-H. Tseng, Appl. Phys. Lett. **96**, 091105 (2010).
[29] W. Klingesten and H. Schweizer, Solid-State Electron. **21**, 1371 (1978).
[30] S.-R. Jan, C.-Y. Chen, C.-H. Lee, S.-T. Chan, K.-L. Peng, C. W. Liu, Y. Yamamoto, and B. Tillack, Appl. Phys. Lett. **98**, 141105 (2011).
[31] J. R. Haynes, Phys. Rev. **98**, 1866 (1955).
[32] M. El Kurdi, T. Kociniewski, T.-P. Ngo, J. Boulmer, D. Débarre, P. Boucaud, J. F. Damlencout, O. Kermarrec, and D. Bensahel, Appl Phys. Lett. **94**, 191107 (2009).
[33] J. R. Haynes, M. Lax, and W. F. Flood, J. Phys. Chem. Solids **8**, 392 (1959).
[34] H. Y. Fan, Phys. Rev. **82**, 900 (1951).
[35] P. B. Allen and M. Cardona, Phys. Rev. B **27**, 4760 (1983).
[36] P. Lautenschlager, P. B. Allen, and M. Cardona, Phys. Rev. B **31**, 2163 (1985).
[37] M. C. Wingert, Z. C. Y. Chen, E. Dechaumphai, J. Moon, J.-H. Kim, J. Xiang, and R. Chen, Nano Lett. **11**, 5507 (2011).
[38] D. Li, Y. Wu, P. Kim, L. Shi, P. Yang, and A. Majumdar, Appl. Phys. Lett. **83**, 2934 (2003).
[39] L. Bergman, X.-B. Chen, J. L. Morrison, J. Huso, and A. P. Purdy, J. Appl. Phys. **96**, 675 (2004).
[40] L. Bergman, X.-B. Chen, J. Feldmeier, and A. P. Purdy, Appl. Phys. Lett. **83**, 764 (2003).
[41] P. A. M. Rodrigues, P. Y. Yu, G. Tamulaitis, and S. H. Risbud, J. Appl. Phys. **80**, 5963 (1996).

[42]P. Parkinson, J. Lloyd-Hughes, Q. Gao, H. H. Tan, C. Jagadish, M. B. Johnston, and L. M. Herz, Nano Lett. **7**, 2162 (2007).
[43]L. V. Titova, T. B. Hoang, J. M. Yarrison-Rice, H. E. Jackson, Y. Kim, H. J. Joyce, Q. Gao, H. H. Tan, C. Jagadish, X. Zhang, J. Zou, and L. M. Smith, Nano Lett. **7**, 3383 (2007).
[44]S. Reitzenstein, S. Munch, C. Hofmann, A. Forchel, S. Crankshaw, L. C. Chuang, M. Moewe, and C. Chang-Hasnain, Appl. Phys. Lett. **91**, 091103 (2007).
[45]R. P. Prasankumar, S. Choi, S. A. Trugman, S. T. Picraux, and A. Taylor, Nano Lett. **8**, 1619 (2008).
[46]D. H. Lindley and P. C. Banbury, Proc. Phys. Soc. London **74**, 395 (1959).
[47]R. H. Kingston, J. Appl. Phys. **27**, 101 (1956).
[48]H. Statz, G. A. de Mars, L. J. Davis, and A. J. Adams, Phys. Rev. **101**, 1272 (1956).
[49]T. Hanrath and B. A. Korgel, J. Phys. Chem. B **109**, 5518 (2005).
[50]Y. Dan, K. Seo, K. Takei, J. H. Meza, A. Javey, and K. B. Crozier, Nano Lett. **11**, 2527 (2011).
[51]J. E. Allen, E. R. Hemesath, D. E. Perea, J. L. Lensch-Falk, Z. Y. Li, F. Yin, M. H. Gass, P. Wang, A. L. Bleloch, R. E. Palmer, and L. J. Lauhon, Nat. Nanotechnol. **3**, 168 (2008).
[52]N. Derhacobian, P. Fine, J. T. Walton, Y. K. Wong, C. S. Rossington, and P. N. Luke, IEEE Trans. Nucl. Sci. **41**, 1026 (1994).
[53]P. H. Brill and R. F. Schwartz, Phys. Rev. **112**, 330 (1958).
[54]W. van Roosbrozck and W. Shockley, Phys. Rev. **94**, 1558 (1954).
[55]W. P. Dumke, Phys. Rev. **105**, 139 (1957).
[56]M. El Kurdi, H. Bertin, E. Martincic, M. de Kersauson, G. Fishman, S. Sauvage, A. Bosseboeuf, and P. Boucaud, Appl. Phys. Lett. **96**, 041909 (2010).
[57]C. Li, Y. Chen, Z. Zhou, H. Lai, and S. Chen, Appl. Phys. Lett. **95**, 251102 (2009).
[58]X. Sun, J. Liu, L. C. Kimerling, and J. Michel, Appl. Phys. Lett. **95**, 011911 (2009).
[59]J. Liu, X. Sun, R. Camacho-Aguilera, L. C. Kimerling, and J. Michel, Opt. Lett. **35**, 679 (2010).
[60]J. Liu, X. Sun, L. C. Kimerling, and J. Michel, Opt. Lett. **34**, 1738 (2009).
[61]X. Sun, J. Liu, L. C. Kimerling, and J. Michel, Opt. Lett. **34**, 1198 (2009).
[62]S. Hu, Y. Kawamura, K. C. Y. Huang, Y. Li, A. F. Marshall, K. M. Itoh, M. Brongersma, and P. C. McIntyre, Nano Lett. **12**, 1385 (2012).